Production Engineering
https://doi.org/10.1007/s11740-022-01141-y

PRODUCTION PROCESS

Investigation of the friction behavior between dry/infiltrated glass fiber fabric and metal sheet during deep drawing of fiber metal laminates

Moritz Kruse[1] · Henrik O. Werner[2,3] · Hui Chen[1] · Thomas Mennecart[4] · Wilfried V. Liebig[2] · Kay A. Weidenmann[5] · Noomane Ben Khalifa[1,6]

Received: 6 April 2022 / Accepted: 3 June 2022

Abstract
During deep drawing processes of fiber metal laminates, such as the newly developed in-situ hybridization process, fibers and metal sheets come into contact while the dry fabric is infiltrated by a reactive matrix system. The viscosity of the matrix increases as polymerization starts during deep-drawing. In the in-situ hybridization process, a dry fiber metal laminate is deep drawn while a thermoplastic matrix system is injected into the glass fiber fabric layer in a resin transfer molding process. During forming of the fiber metal laminate, friction occurs in tangential direction to the metal sheet. The friction plays the main role in preventing the elongation of the sheets in the deep drawing process. Therefore, the measurement of friction coefficients between fibers and metal sheets is essential. In this paper, the friction between sheet metal and dry or infiltrated glass fiber fabric under high contact pressures of 1.67 MPa, as occurring in deep drawing processes, is characterized. A modified strip drawing test setup is used to analyze the coefficient of friction under a constant high contact pressure. Compression tests were performed to show that Coulomb friction can be assumed. Different types of glass fiber fabrics and liquids with defined viscosities are used. It was found that fluids with higher viscosity decrease the friction coefficients in the interface, which is physically explained. For the in-situ hybridization process, it is deduced that with low viscosities, a better infiltration is achieved, while higher viscosities reduce the friction coefficient for better formability.

Keywords Fiber metal laminates · Friction coefficient · Metal-fabric friction · In-situ hybridization

1 Introduction

The increasing demand for high-performance and lightweight structures has promoted the application of fiber metal laminates (FML) in the aircraft industry over the last decades. FMLs consist of thin metal layers alternated with composite layers, e.g. ARALL (aramid fiber reinforced aluminum laminate), GLARE (glass fiber reinforced aluminum laminate), and CARALL (carbon fiber reinforced aluminum laminate) [1]. By using FML, advantageous properties can be achieved and the disadvantages of monolithic materials or structures can be compensated. Thus, high crack propagation resistance [2], high absorption energy [3], good corrosion resistance and resistance to flammability [4] can be achieved [5]. Important applications can be found in the transportation sector, e.g., in aviation [6] or increasingly in the automotive sector [7]. Structural components made of FMLs were initially produced by the autoclave process [8]. In this process, metal sheets are stacked alternately with

At the time of the experiments, Thomas Mennecart was employed as research assistant at the Institute of Forming Technology and Lightweight Components (Technical University of Dortmund).

✉ Moritz Kruse
moritz.kruse@leuphana.de

1 Institute of Product and Process Innovation, Leuphana University of Lüneburg, Lüneburg, Germany

2 Institute for Applied Materials, Karlsruhe Institute of Technology (KIT), Karlsruhe, Germany

3 Institute of Vehicle System Technology, Karlsruhe Institute of Technology (KIT), Karlsruhe, Germany

4 Ettringen, Germany

5 Institute of Materials Resource Management, University of Augsburg, Augsburg, Germany

6 Institute of Materials and Process Design, Helmholtz-Zentrum Hereon, Geesthacht, Germany

Published online: 22 June 2022

the pre-impregnated fibers. These layers are then evacuated, placed in an autoclave and cured under high pressure (0.5–0.6 MPa) and elevated temperature (about 120 °C) [9]. Only small curvatures, as in an aircraft fuselage, can be realized in an autoclave process [10]. Various manufacturing processes have been developed to manufacture FML components of higher complexity: (a) by using a resin injection process with an asymmetrical structure [11]; (b) by using a preimpregnated (prepreg) and a preformed sheet [12]; (c) by using a semi-finished product consisting of pre-consolidated prepreg and adhering cover sheets [13]. Due to these usually expensive fabrication processes and low formability, FMLs have not yet become widely used in large-scale production.

The newly developed in-situ hybridization process for the production of FML shows great potential to produce three-dimensional structural components in the car body-in-white in one step with one forming tool [14]. During the deep drawing of the dry FML, the fabric layers are infiltrated with a reactive thermoplastic matrix system in a thermoplastic resin transfer molding (T-RTM) process. An advantage of the process is the use of inexpensive semi-finished products and a very low viscosity matrix, which allows infiltration of fibers in regions of low cross-section and high fiber volume content [15]. Due to the low viscosity of the in-situ injected matrix, the fibers are in direct contact with the sheets throughout the forming process [16]. The permanent contact of fibers and sheet, as well as the higher contact pressures than in the state of the art, lead to reduced formability of the sheets due to friction [16]. Therefore, the friction between the fabric and the metal sheet has to be investigated specifically.

Usually, Coulomb friction is assumed. However, Howell [17] found that the coefficient of friction at low contact pressures for fibers is higher than at high contact pressures. Howell cites the contact state at the surface of the friction partners as the reason. At high contact pressures, plastic contact of the surface irregularities occurs, leading to Coulomb's friction equation

$$F = \mu N, \tag{1}$$

which is a special case of the more general relationship

$$F = kN^n \tag{2}$$

formulated by Bowden and Young in 1951 [18]. Here, F is the friction force, N the normal load, μ the coulomb friction value and k, n curve fitting parameters for non-linear, normal load dependent friction. For contact with entirely plastic deformation of the friction partners, $n=1$ is assumed to be identical to Coulomb's friction equation. For contact with pure elastic deformation of the friction partners $n=2/3$ is valid. Values between $n=2/3$ and $n=1$ indicate the fraction of plastic contact. According to Howell, the contact state of friction partners depends on the real contact area and the yield strength under compression due to the normal load. The coefficient of friction then results from the shear strength of the welded surface irregularities.

Draping dry or impregnated fibers for the manufacturing of fiber-reinforced composites does not require high normal forces in the direction of fabric thickness. Therefore, metal-fabric friction was previously investigated only under low normal forces to characterize the friction behavior between ply and tool. Sachs et al. [19] summarized different test methods for characterizing dynamic friction between fabrics and metal surfaces, where the maximum contact pressure was $p=0.16$ MPa. In a common test method, a weighted sled is pulled over a test bed to determine the friction between ply/ply or tool/ply [20]. Another commonly applied test setup uses a plate with fabric attached to it, that is pulled out of or through two pressure plates where the other friction partner is attached to [21]. Rigidity of the tool is important, as misalignment of the tool due to the friction force can lead to uneven pressure distribution and therefore wrong measurements [19]. For dry fabrics, the ply/ply and tool/ply friction can usually assumed to be independent of the drawing velocity and normal load [22]. When infiltrating the fabric with a viscous matrix, friction decreases as the matrix acts as lubrication. Furthermore, the friction behavior becomes dependent on the drawing velocity and normal load when introducing a viscous matrix. With increasing drawing velocities and decreasing normal loads, the friction increases [23]. Opposing views exist, whether the influence of the drawing velocity or the normal load on the coefficient of friction is higher [24]. In the forming of FMLs, much higher normal loads than in the fabrication of fiber-reinforced composites are occurring on the interface between metal sheet and fabric. As the normal pressure increases, the area of the fabric in contact with the friction partner increases [25]. The area increases due to the reorientation of the fibers as a result of the normal pressure. This process-induced pressure thus affects the movement of the fibers in the semi-finished product (e.g. fabric). This is shown by the investigations of Samadi and Robitaille [26] with a numerical model, to what extent the contact area increases with increasing compaction of the fibers. From initial point contact, the contact area increases due to compaction and results in a higher fiber volume content. Yousaf et al. [27] state that the increase in area is caused by reorientations and by superimposed fibers sliding into the free spaces. Thus, when pressure is applied in the direction of fabric thickness, the thickness of the fabric decreases.

So far, there is no standardized strategy to measure the friction between sheet metal and dry or infiltrated fabric under high contact pressures, like $p=2$ MPa. This article presents the experimental characterization of the friction coefficient using a modified strip drawing test. In this test

setup, high contact pressures can be realized. The aim of the investigations is to find friction pairings that reduce friction and thereby increase formability in the in-situ hybridization process.

2 Material and experimental methods

2.1 Material

Different types of glass fibers and of metal sheets are selected to analyze the friction coefficients. The aluminum alloy AA 5182-H111 and cold rolled DC04 sheet metal blank with a thickness of 1.0 mm are common materials for body-in-white in the automotive industry. The metal sheets have a surface roughness of approximately $R_a = 1\,\mu m$. Two fabrics with different weave types, plain woven fabric and twill woven fabric, are selected to investigate the influence of the weave type under load (Fig. 1). In order to investigate the influence of the laminate thickness and the geometry, which affects the weight per unit area, on the fabric under load, two different weights per unit area are selected for the twill woven fabric: 80 g/m^2 and 280 g/m^2. The plain woven fabric has a weight of 280 g/m^2.

2.2 Flat strip drawing test

The flat strip drawing tests are carried out on a test facility as described by Mennecart [15] and shown in Fig. 2. The sheet metal strip is clamped between two friction elements, whereby a defined force F is applied in the normal direction. The two specimens with a contact area of 30 mm (width) × 40 mm (height) = 1200 mm^2 are covered with a layer of the glass fabric to be examined. The sheet metal strips used have a length of 300 mm and a width of 40 mm. The sheet metal strip is pulled at a constant velocity v while the compaction force N in thickness direction is kept constant and the pulling force F is measured. The applied transverse force and the drawing velocity are controlled. The forces are measured by piezo load cells (type 0911A

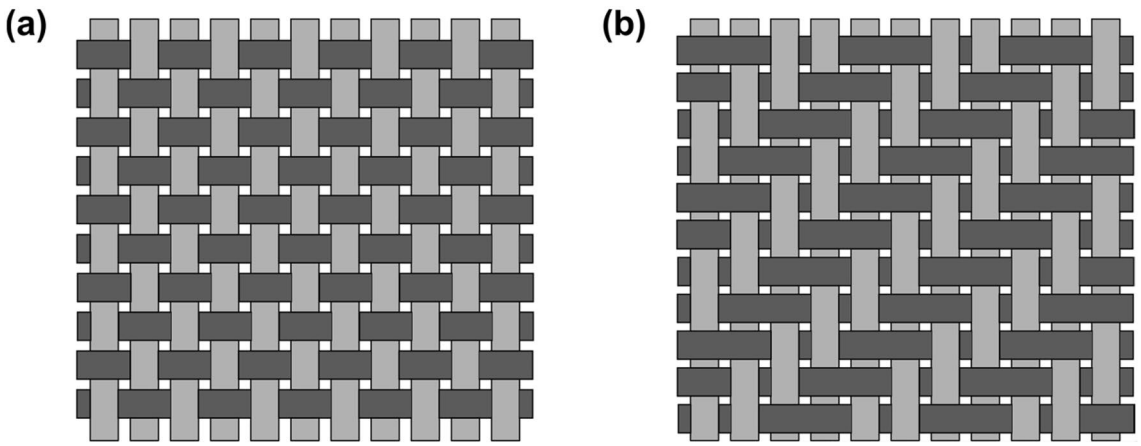

Fig. 1 Geometries of the fabric: **a** plain woven fabric; **b** twill woven fabric

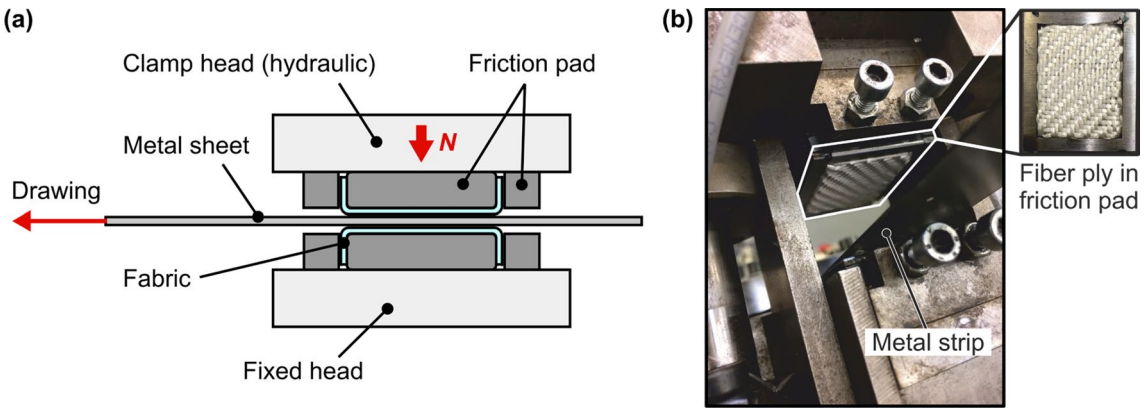

Fig. 2 Strip drawing test setup: **a** schematic sketch of the test principle; **b** specimen in the test setup

0–15 kN in drawing direction and type 9021A 0–35 kN in clamping direction) from Kistler. The displacement is determined by using a potentiometric position transducer from Novotechnik (type LWH-0200). Assuming Coulomb friction, the following formula is used to obtain the dynamic coefficient of friction μ_D:

$$\mu_D = \frac{F}{2N} \tag{3}$$

The strip is clamped with a force of 2000 N, which corresponds to a contact pressure of $p = 1.67$ MPa, and pulled at a velocity of 600 mm/min. The determination of the coefficient of friction ends after five seconds. In order to detect an influence on the fiber orientation, the coefficients of friction for fibers which are clamped in 0°/90° and in ± 45° are determined as shown in Fig. 3a.

Substitute fluids of different dynamic viscosities are used to determine the influence of viscosity on the coefficient of friction, because the reactive matrix system would polymerize and change its viscosity while testing. Silicone oils with viscosities of 160 mPa s, 10,000 mPa s and 100,000 mPa s are used. The viscosity of the low viscous oil corresponds to the initial viscosity of the matrix system used in deep drawing of fiber metal laminate with in-situ hybridization. With the current in-situ hybridization process, the deep drawing is completed after 90 s with a low viscous matrix. With lower drawing velocities, the matrix would polymerize further during the deep drawing. Higher viscosities are intended to reflect the increase in viscosity during polymerization, as shown in Fig. 4. The fabrics are completely infiltrated with the oils. Excess oil is pressed out by the contact pressure. Three to four evaluable tests for each configuration are carried out.

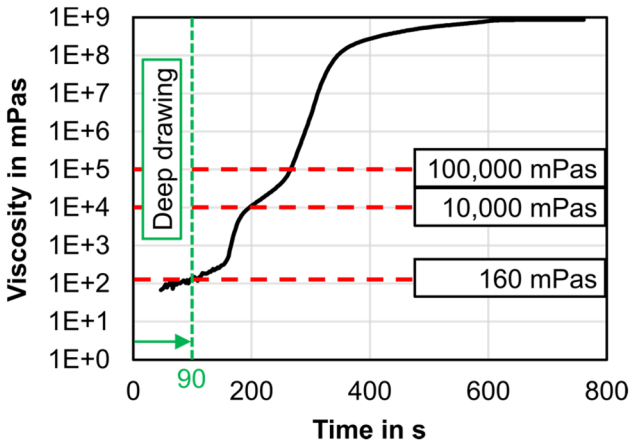

Fig. 4 Viscosity of the matrix over time at 80 °C and substitutive viscosities chosen for friction tests

3 Results

3.1 Friction coefficient between fabric/sheet metal in strip drawing test

Figure 5 shows a selection of the coefficients of friction of the dry and infiltrated fabrics for a fiber orientation of 0°/90° to the drawing direction of the sheets against the displacement. The mean values and standard deviations of all evaluable tests are plotted to compare different fabric and metal types under the influence of oils with different viscosities. The dry fabric in interaction with both the AA 5182-H111 and DC04, respectively, shows the highest friction. With up to $\mu = 0.23$, this is the highest value for the heavy twill woven fabric and the plain woven fabric. The friction coefficients are similar for the combination with DC04 and with

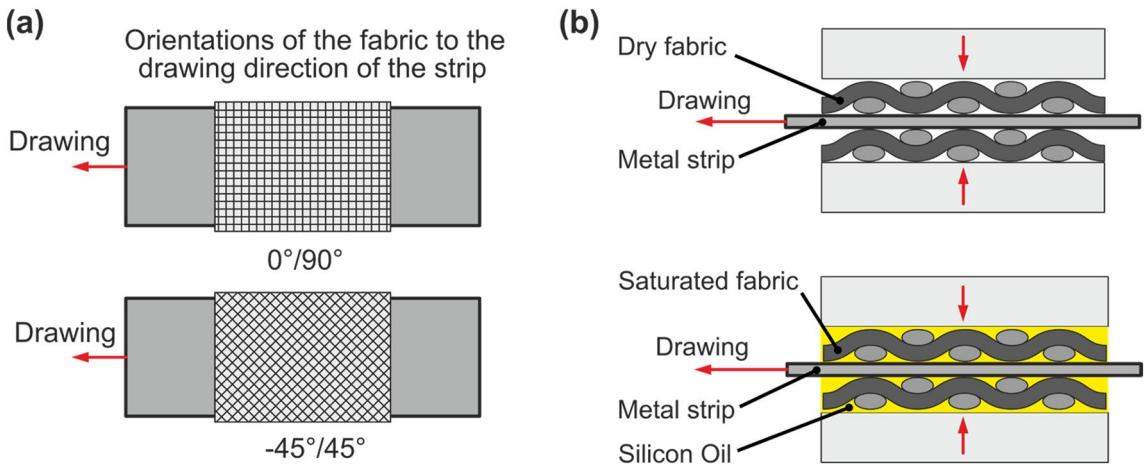

Fig. 3 Test conditions of the strip drawing: **a** orientations of the fiber ply; **b** dry and infiltrated state

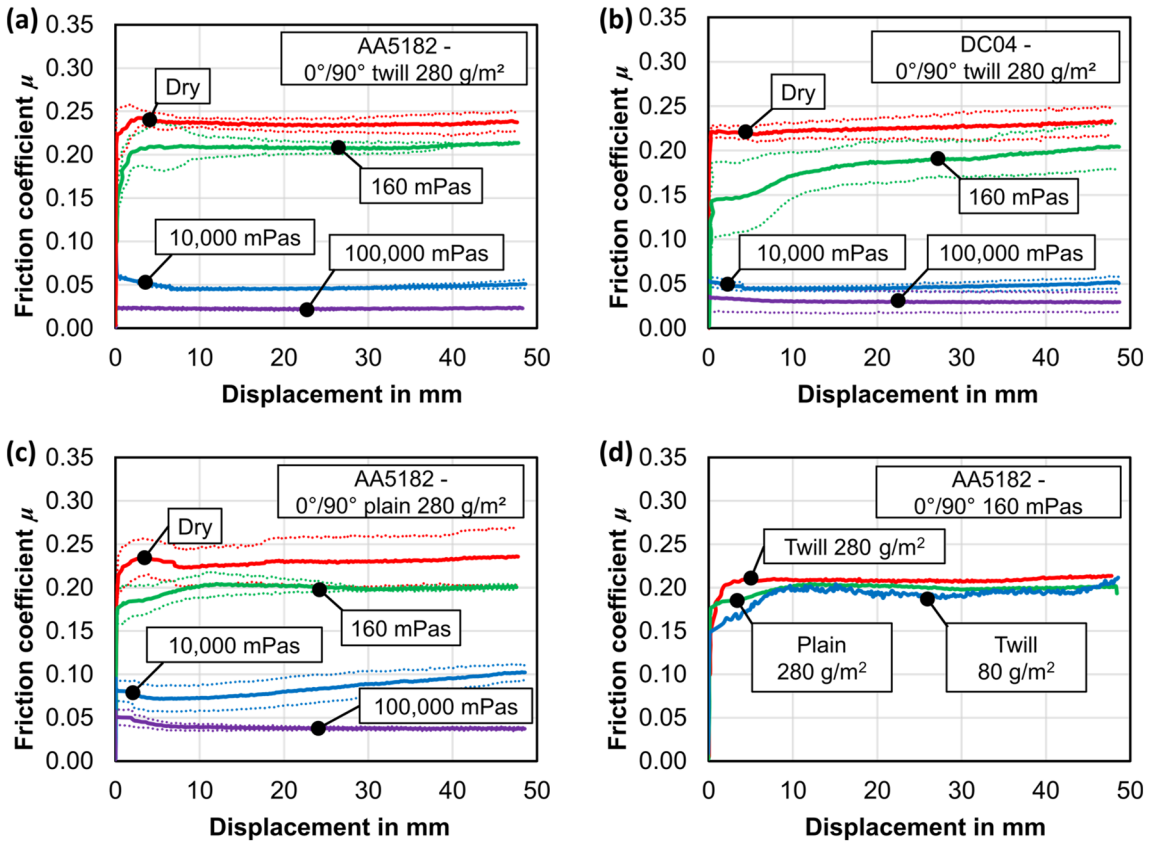

Fig. 5 Friction coefficient in 0°/90° direction of the fabric (standard deviations shown with dotted lines): **a** between AA5182 sheet and twill woven fabric 280 g/m^2; **b** between DC04 and twill woven fabric 280 g/m^2; **c** between AA5182 and plain woven fabric 280 g/m^2; **d** between AA5182 sheet and different fabrics infiltrated by 160 mPa s viscous fluid (no standard deviation shown for better visibility)

AA 5182-H111. The coefficient of friction drops slightly by approx. 0.03 in the wet condition with 160 mPa s oil compared to the dry state. The friction in dry state and with 160 mPa s viscous oil is mostly independent of the fabric typ. With higher viscous oils, the friction coefficient is much lower. The friction associated with the oil with a viscosity of 10,000 mPa s produces contact friction coefficients between $\mu = 0.05$ (light twill woven fabric) and $\mu = 0.12$ (plain woven fabric). At 10,000 mPa s viscosity, a sharp increase in the friction coefficient during the draw path for the friction pairing of plain woven fabric and sheet metal can be noticed. The coefficient of friction increases from an initial value of $\mu = 0.07$ to $\mu = 0.12$. This effect is not observed for the twill woven fabric at 10,000 mPa s in combination with the AA5182-H111. Here, the friction coefficient is slightly lower ($\mu = 0.05$) than for the plain woven fabric and steady over the displacement. However, a similar effect is observed in the twill woven fabric in combination with DC04 at 160 mPa s, where the initial friction coefficient is lower than in combination with AA5182-H111 but increases to the same value at further displacement. The coefficient of friction is lowest in the case of the friction pairing between fibers infiltrated with the highly viscous oil (100,000 mPa s) and the sheet metal. Here, the coefficient of friction is between $\mu = 0.02$ and $\mu = 0.04$. Again, the friction coefficient is slightly lower for the twill woven fabric. It is steady over the displacement for both plain and twill woven fabric at 100,000 mPa s. Standard deviations are around ± 10% for most material combinations with slightly higher deviations for DC04 with twill woven fabric and 160 mPa s as well as 100,000 mPa s viscous oil. Higher deviations in these cases are caused by considerably higher (for 160 mPa s) or lower (for 100,000 MPa) measured friction coefficients in one of the three performed tests. They were not excluded from the analysis as outliers as they are still in a reasonable range.

Figure 6 shows the coefficients of friction for the dry and for the infiltrated fabrics for a fiber orientation of ± 45° to the drawing direction of the sheet. In general, the friction shows a similar behavior in ± 45° direction as in 0°/90° direction. The friction coefficients are higher for dry fabrics and decrease with increasing viscosity. Friction coefficients are slightly higher in ± 45° direction, in particular for the twill woven fabric. Smaller differences can be observed for the plain woven fabric, where the main difference is an even

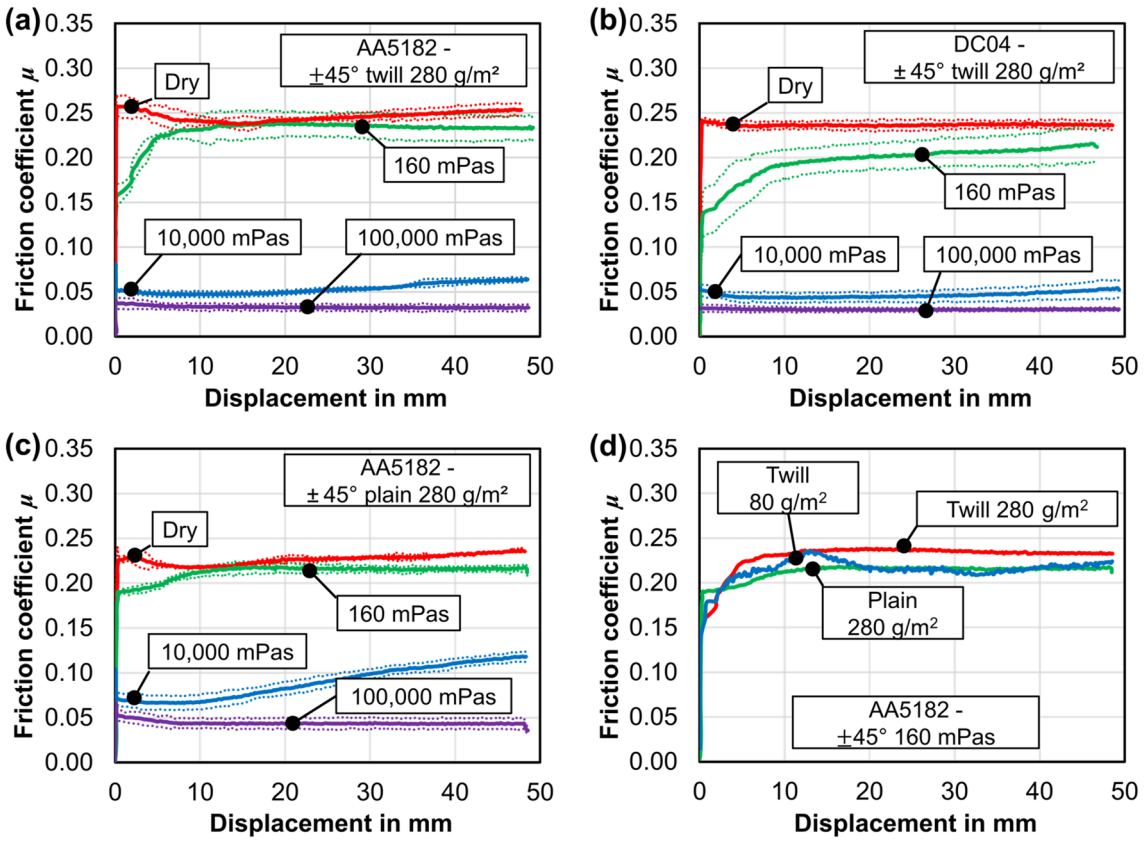

Fig. 6 Friction coefficient in ± 45° direction of the fabric (standard deviations shown with dotted lines): **a** between AA5182 sheet and twill woven fabric 280 g/m^2; **b** between DC04 and twill woven fabric 280 g/m^2; **c** between AA5182 and plain woven fabric 280 g/m^2; **d** between AA5182 sheet and different fabrics infiltrated by 160 mPa s viscous fluid (no standard deviation shown for better visibility)

larger increase of the friction coefficient over the displacement for the fabric that is infiltrated with the 10,000 mPa s oil. For the twill woven fabric, a sharp increase in friction coefficient can be seen during the initial displacement in combination with the 160 mPa s oil and both DC04 and AA5182-H111. In 0°/90° direction, this increase is not observed in combination with AA5182-H111 except for a small increase in the very beginning, whereas in combination with DC04, the increase in friction coefficient is spread out place over the whole displacement length. Similar to the experiments conducted in 0°/90°-direction, the standard deviations are around ± 10% or lower. Standard deviations are slightly lower for the experiments performed in ± 45° direction.

4 Discussion

4.1 Fabric compression test to verify the application of Coulomb's law

One compression test from 0.005 to 5 MPa was performed on three layers of the twill woven fabric 280 g/m^2 to verify the assumption of contact with plastic deformation for the application of Coulomb's friction law. The initial thickness of the fabric at 0.005 MPa amounts to 0.32 mm. The compression behavior is assumed to be similar for the plain woven fabric 280 g/m^2 and twill woven fabric 80 g/m^2. The obtained thickness-pressure curve is shown in Fig. 7. According to Yousaf et al. [27], it consists of three parts. First a linear part and second an exponential part, where the majority of the compression takes place by rearranging of the fibers and interlayer nesting. The last part of the compression curve is determined by the elastic deformation of the fibers itself as almost all possible nesting took place at lower compression loads. For the tested fabric, this is the case for pressures higher than approximately 1 MPa. Bowden and Young's friction is dependent on the contact

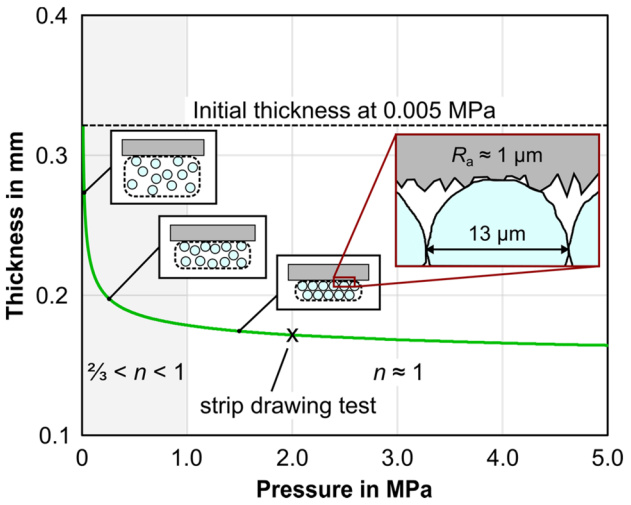

Fig. 7 Thickness-pressure curve of one fiber layer for the compression of three layers twill woven fabric 280 g/m^2 and schematic overview of the compression behavior of one fiber roving in contact with the metal sheet

area and type of contact between the friction partners. At high pressures, the contact area between metal sheet and fibers can be seen as constant, since only very little elastic deformation is occurring in the brittle and stiff glass fibers. The contact between metal sheet and glass fibers can be seen as almost entirely plastic. While the glass fibers should exhibit almost no deformation compared to the metal sheets, the deformation of the surface irregularities on the metal sheet should be almost entirely plastic at high pressures as they are occurring in the in-situ hybridization process and the strip drawing tests. Coulomb friction [with $n = 1$ in Eq. (2)] can therefore be assumed. Under low contact pressures, Coulomb's law could not be applied for the determination of the friction coefficient because the change in contact area would have to be considered.

4.2 Interaction between fabric/sheet metal in strip drawing test

The standard deviations of approximately ± 10% are low compared to the differences observed for different material combinations. The number of tests carried out can therefore assumed to be sufficient for this investigation. Slightly lower standard deviations were observed in ± 45° direction. Although being almost the same in warp and weft direction (133 g/m^2 and 143 g/m^2), a slight anisotropy in the fabric might lead to small differences between 0° and 90° direction that could explain the higher deviations. The friction coefficient measurements for the dry fabrics and for the fabrics infiltrated with the low viscous fluid show that the friction coefficients are approx. 0.01 to 0.02 higher when the fiber orientation is ± 45°. A possible cause of friction in fiber metal contact could be that the fibers rotate in the direction of tension due to friction (Fig. 8). Due to less undulations and better drapability, a greater rotation of the roving in the twill woven fabric compared with plain woven fabric is to be expected. For the fiber rotation, additional force is needed which explains the measured higher friction coefficient for fabrics in ± 45° direction. At the crossing points of the rovings, the contact pressure is much higher than the average pressure.

For some specimens, an increase in the friction coefficient can be observed with further displacement. This effect occurs in particular for the ± 45° fiber orientation to the drawing direction. This can be explained by the fact that the liquid is quickly discharged to the outside in a V-shape, as Hahn et al. [11] also found in bending processes. A faster squeezed out fluid leads to an increasing number of fibers interacting with the metal sheet and a continuously increased coefficient of friction (Fig. 9). Without fluid, the contact pressure is very high at the crossing points of the fabric. Because the matrix is transported forward with a fiber orientation of 0°/90°, the fluid is not as easily squeezed out of the fabric. The displacement of the fluid is also more difficult with medium viscosity. The matrix film is dragged along before displacement of the fluid occurs over time. This means that the friction coefficient in this case changes from a low to a higher value. Using a highly viscous fluid, no matrix is squeezed out and the matrix is in contact with the sheet during the entire draw path. With increasing viscosity, the pressure is more evenly distributed and gets closer to the average area pressure. As a result, the friction factor is low when the viscosity is high.

The influence of fluids with different viscosities on the friction between fabric and metal was investigated under a high normal pressure. Dry friction without viscous matrix is independent of the drawing velocity. However, when using a viscous matrix, the friction decreases with decreasing velocity. In this work, a high drawing velocity of 600 mm/min was investigated. For lower drawing velocities, as occurring in the in-situ hybridization process, the difference in friction between dry and infiltrated fabrics is therefore assumed to be even higher.

As of now, a low reactive matrix system is used in the in-situ hybridization process. During the deep drawing process, only little polymerization takes place with increasing matrix viscosity from initial 100 mPa s to approximately 200–300 mPa s [14], as shown in Fig. 4. Most of the viscosity increase takes place during polymerization when holding the position after deep drawing. This investigation shows that lower friction values hinder the metal sheet less in the forming process and allow greater degrees of forming. As lower frictions can be achieved with a higher viscous matrix, lower drawing velocities or using a matrix system with faster polymerization time could improve the forming behavior in the in-situ

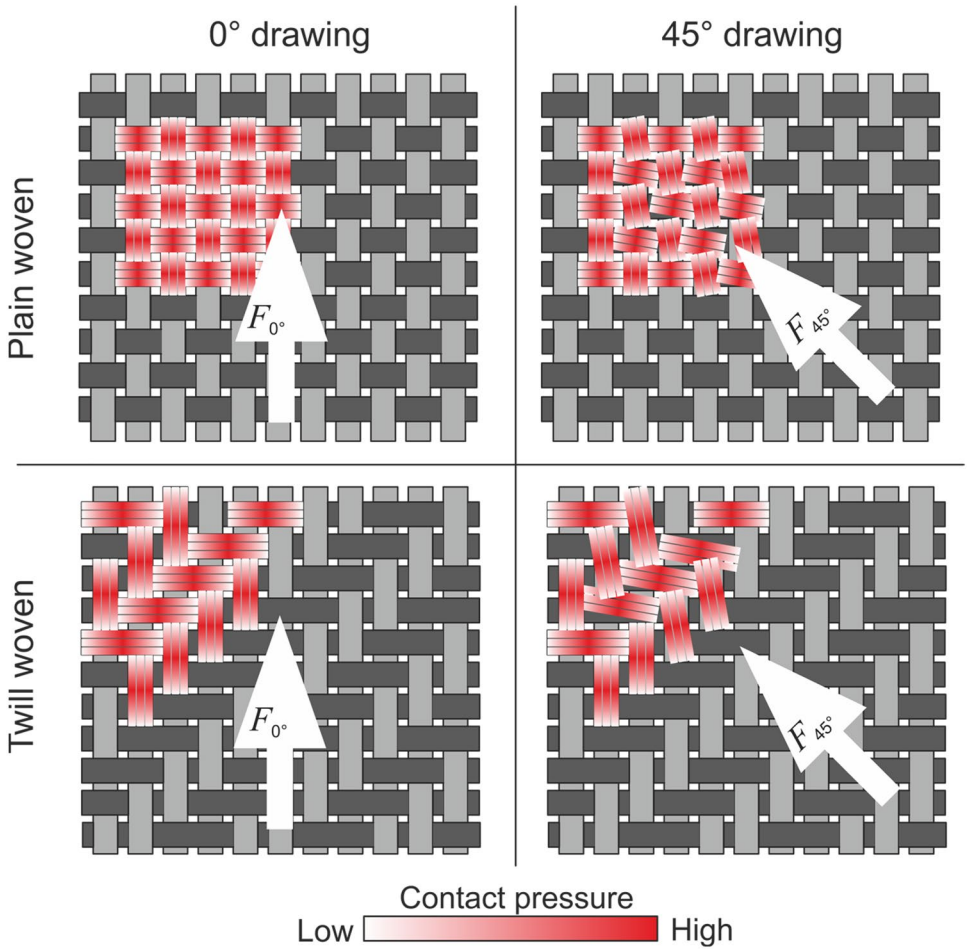

Fig. 8 Schematic illustration of the fiber behavior due to friction between sheet metal and fibers

hybridization process. When polymerization already takes place during the forming process, the friction is reduced due to higher matrix viscosity, in particular towards the end of the forming process. However, a high viscosity is also counterproductive for forming of the fabric layer, as other studies have shown [28]. High viscosities reduce the friction between fabric and metal sheet, but lead to higher fluid forces. The higher fluid forces lead to fiber washing and thus poorer forming results in the fabric due to fiber misorientation. Therefore, further research has to be conducted to find a process window for the in-situ hybridization process.

5 Conclusion

The coefficient of friction was measured by strip drawing tests between glass fiber fabrics and metal sheets of aluminum and steel. For a characterization close to the process, it is essential to represent the friction parameters required in a realistic way. For low contact pressures the non-linear friction behavior has to be accounted for. For high contact pressures, as they occur in the in-situ hybridization process, it could be shown that the strip drawing test is suitable. It was shown that the applied contact pressures were high enough to assume Coulomb friction. The following conclusions regarding the friction coefficient for different material combinations can be drawn:

- The friction coefficient in fiber-metal combinations is mainly dependent on the lubrication due to infiltration with matrix.
- The friction between fabric and metal is highest for dry fabrics due to high local contact pressure at the crossing points of the rovings.
- Infiltrated fabrics show a lower friction coefficient as the fluid leads to a more even pressure distribution in particular with higher viscous oils. Therefore, higher viscous fluids reduce the friction between metal and fabric. With increasing drawing length, the friction coefficient also depends on the displacement of the fluid out of the fabric.
- The fluid is more easily discarded in $\pm 45°$ direction as the rovings are rotated by the drawing force. Thus, friction coefficients are slightly higher in $\pm 45°$ direction.

The results of the strip drawing test demonstrate that a higher viscous matrix is more favorable for metal sheet

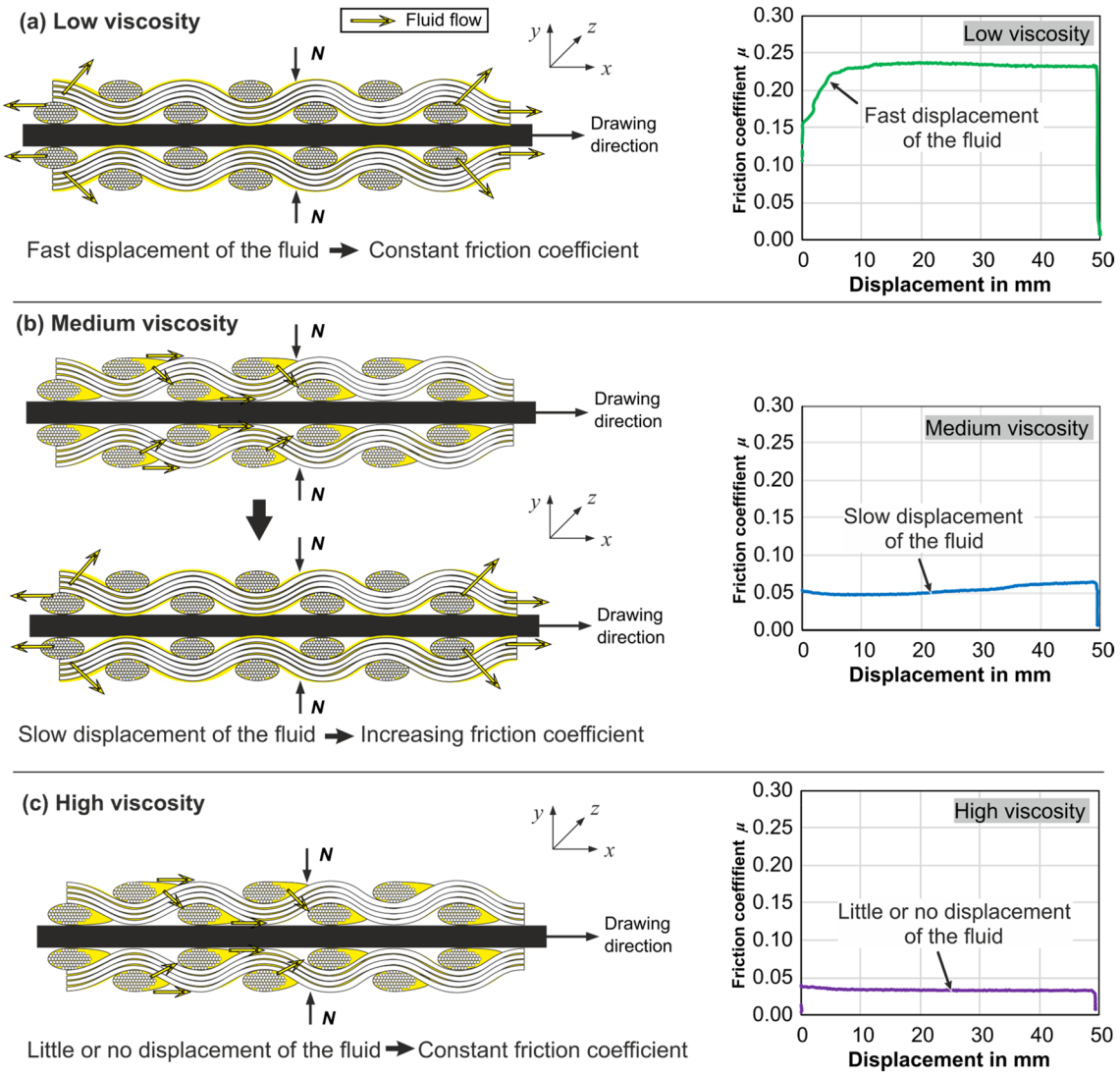

Fig. 9 Matrix displacement for infiltrated fibers in contact with moving sheet at: **a** low viscosity; **b** medium viscosity; **c** high viscosity of the matrix

forming, since it leads to lower friction values. In the in-situ hybridization process, forming takes place with a low viscous matrix. Polymerization during the forming process might improve the forming behavior by increasing the viscosity towards the end of the forming process. However, high viscosities are counterproductive for the forming of the fabric, as they can lead to fiber washing and misorientation due to high fluid forces. A compromise between low friction but no fiber misorientation has to be found for improving the forming process of FMLs.

Author contributions MK: investigation, resources, formal analysis, data curation, writing—original draft, writing—review and editing, visualization, project administration; HOW: conceptualization, writing—review and editing, project administration; HC: writing—original draft, writing—review and editing, visualization; TM: conceptualization, methodology, investigation, resources, formal analysis, data curation, visualization, project administration; WVL: writing—review and editing, supervision; KAW: funding acquisition, supervision; NBK: funding acquisition, supervision.

Funding Open Access funding enabled and organized by Projekt DEAL. The authors would like to thank the German Research Foundation (DFG) for funding the projects BE 5196/4-1, BE 5196/4-2 and WE 4273/13-1, WE 4273/13-2.

Declarations

Conflict of interest The authors declare no conflict of interest.

References

1. Vlot A (2001) Glare: history of the development of a new aircraft material. Kluwer Academic Publishers, Dordrecht. https://doi.org/10.1007/0-306-48398-X
2. Khan SU, Alderliesten RC, Benedictus R (2011) Delamination in fiber metal laminates (GLARE) during fatigue crack growth under variable amplitude loading. Int J Fatigue 33:1292–1303. https://doi.org/10.1016/j.ijfatigue.2011.04.002
3. Vlot A, Kroon E, La Rocca G (1997) Impact response of fiber metal laminates. KEM 141–143:235–276. https://doi.org/10.4028/www.scientific.net/KEM.141-143.235
4. Hooijmeijer P, Vlot A (2001) Fibre metal laminates exposed to high temperatures. In: Proceedings 13th international conference on composite materials
5. Krishnakumar S (1994) Fiber metal laminates—the synthesis of metals and composites. Mater Manuf Process 9:295–354. https://doi.org/10.1080/10426919408934905
6. Pacchione M, Telgkamp J (2006) Challenges of the metallic fuselage. In: 25th congress of international council of the aeronautical sciences, Hamburg
7. Dröder K, Vietor T (eds) (2019) Technologies for economical and functional lightweight design. Springer, Berlin https://doi.org/10.1007/978-3-662-58206-0
8. Sinke J (2003) Manufacturing of GLARE parts and structures. Appl Compos Mater 10:293–305. https://doi.org/10.1023/A:1025589230710
9. Park SY, Choi WJ, Choi HS, Kwon H (2010) Effects of surface pre-treatment and void content on GLARE laminate process characteristics. J Mater Process Technol 210:1008–1016. https://doi.org/10.1016/j.jmatprotec.2010.01.017
10. Kim SY, Choi WJ, Park SY (2007) Spring-back characteristics of fiber metal laminate (GLARE) in brake forming process. Int J Adv Manuf Technol 32:445–451. https://doi.org/10.1007/s00170-005-0355-8
11. Hahn M, Ben Khalifa N, Weddeling C, Shabaninejad A (2016) Springback behavior of carbon-fiber-reinforced plastic laminates with metal cover layers in V-die bending. J Manuf Sci Eng. https://doi.org/10.1115/1.4034627
12. Behrens B-A, Hübner S, Neumann A (2014) Forming sheets of metal and fibre-reinforced plastics to hybrid parts in one deep drawing process. Procedia Eng 81:1608–1613. https://doi.org/10.1016/j.proeng.2014.10.198
13. Dau J, Lauter C, Damerow U, Homberg W, Tröster T (2011) Multi-material systems for tailored automotive structural components. In: Proceedings 18th international conference on composite materials
14. Mennecart T, Werner H, Ben Khalifa N, Weidenmann KA (2018) Developments and analyses of alternative processes for the manufacturing of fiber metal laminates. In: Volume 2: materials; joint MSEC-NAMRC-manufacturing USA. American Society of Mechanical Engineers. https://doi.org/10.1115/MSEC2018-6447
15. Mennecart T (2022) In-situ Hybridisierung von Faser-Metall Laminaten. Dissertation. Shaker, Reihe Dortmunder Umformtechnik, Band 116. ISBN 978-3-8440-8566-2
16. Mennecart T, Gies S, Ben Khalifa N, Tekkaya AE (2019) Analysis of the influence of fibers on the formability of metal blanks in manufacturing processes for fiber metal laminates. JMMP 3:2. https://doi.org/10.3390/jmmp3010002
17. Howell HG, Mazur J (1953) Amontons' law and fibre friction. J Text Inst Trans 44:T59–T69. https://doi.org/10.1080/19447025308659728
18. Bowden FP, Young JE (1951) Friction of diamond, graphite, and carbon and the influence of surface films. Proc R Soc Lond A 208:444–455. https://doi.org/10.1098/rspa.1951.0173
19. Sachs U, Akkerman R, Fetfatsidis K, Vidal-Sallé E, Schumacher J, Ziegmann G, Allaoui S, Hivet G, Maron B, Vanclooster K, Lomov SV (2014) Characterization of the dynamic friction of woven fabrics: experimental methods and benchmark results. Compos A Appl Sci Manuf 67:289–298. https://doi.org/10.1016/j.compositesa.2014.08.026
20. Page J, Wang J (2000) Prediction of shear force and an analysis of yarn slippage for a plain-weave carbon fabric in a bias extension state. Compos Sci Technol 60:977–986. https://doi.org/10.1016/S0266-3538(99)00198-0
21. Pasco C, Khan M, Gupta J, Kendall K (2019) Experimental investigation on interply friction properties of thermoset prepreg systems. J Compos Mater 53:227–243. https://doi.org/10.1177/0021998318781706
22. Rashidi A, Montazerian H, Yesilcimen K, Milani AS (2020) Experimental characterization of the inter-ply shear behavior of dry and prepreg woven fabrics: significance of mixed lubrication mode during thermoset composites processing. Compos A Appl Sci Manuf 129:105725. https://doi.org/10.1016/j.compositesa.2019.105725
23. Kim J-Y, Hwang Y-T, Baek J-H, Song W-Y, Kim H-S (2021) Study on inter-ply friction between woven and unidirectional prepregs and its effect on the composite forming process. Compos Struct 267:113888. https://doi.org/10.1016/j.compstruct.2021.113888
24. Nuruzzaman DM, Chowdhury MA, Rahman MM, Kowser MA, Roy BK (2015) Experimental investigation on friction coefficient of composite materials sliding against SS 201 and SS 301 counterfaces. Procedia Eng 105:858–864. https://doi.org/10.1016/j.proeng.2015.05.106
25. Cornelissen B, Sachs U, Rietman B, Akkerman R (2014) Dry friction characterisation of carbon fibre tow and satin weave fabric for composite applications. Compos A Appl Sci Manuf 56:127–135. https://doi.org/10.1016/j.compositesa.2013.10.006
26. Samadi R, Robitaille F (2014) Particle-based modeling of the compaction of fiber yarns and woven textiles. Text Res J 84:1159–1173. https://doi.org/10.1177/0040517512470200
27. Yousaf Z, Potluri P, Withers PJ (2017) Influence of tow architecture on compaction and nesting in textile preforms. Appl Compos Mater 24:337–350. https://doi.org/10.1007/s10443-016-9554-8
28. Bodaghi M, Lomov SV, Simacek P, Correia NC, Advani SG (2019) On the variability of permeability induced by reinforcement distortions and dual scale flow in liquid composite moulding: a review. Compos A Appl Sci Manuf 120:188–210. https://doi.org/10.1016/j.compositesa.2019.03.004